Visualizing pair formation on the atomic scale and the search for the mechanism of superconductivity in high-T_c cuprates

2009 J. Phys.: Condens. Matter 21 164214

(http://iopscience.iop.org/0953-8984/21/16/164214)

J. Phys.: Condens. Matter **21** (2009) 164214 (9pp) doi:10.1088/0953-8984/21/16/164214

Visualizing pair formation on the atomic scale and the search for the mechanism of superconductivity in high-T_c cuprates

A Yazdani

Joseph Henry Laboratories and Department of Physics, Princeton University, Princeton, NJ 08540, USA

E-mail: yazdani@princeton.edu

Received 27 January 2009
Published 31 March 2009
Online at stacks.iop.org/JPhysCM/21/164214

Abstract

We have developed several new experimental techniques, based on the scanning tunneling microscope, to visualize the process of pair formation on the atomic scale and to probe with high precision what controls the strength of pairing in high-T_c cuprate superconductor compounds. These new experiments provide evidence that pairing in these exotic superconductors occurs above the bulk transition temperature and in nanoscale regions with sizes of 1–3 nm. The high temperature nucleation and proliferation of these nanoscale puddles have a strong connection to the temperature–doping phase diagram of these superconductors. On average we have found that the pairing gap Δ and the temperature at which they first nucleate T_p follow the simple relation: $2\Delta/k_BT_p \sim 8$. Moreover, the variations of the pairing strength on the nanoscale can be examined to find microscopic clues to the mechanism of pairing. Specifically, we have found evidence that suggests that strong electronic correlation, as opposed to coupling of electrons to bosons, is responsible for the pairing mechanism in the cuprates. Surprisingly, we have found that nanoscale measurements of electronic correlations in the normal state (at temperatures as high as twice T_c) can be used to predict the strength of the local pairing interaction at low temperatures.

(Some figures in this article are in colour only in the electronic version)

1. Introduction

After more than 20 years of work, the mechanism of pairing and the temperature at which Cooper pairs first form in high temperature copper oxide superconductors are both still hotly debated. Do pairs form at the critical temperature as in conventional superconductors? Is pairing mediated by bosonic excitations, as in conventional BCS superconductors, or is pairing with d-wave symmetry an unavoidable consequence of strong Coulomb repulsion in these compounds? Related to these questions about the nature of the pairing mechanism is the mystery of the pseudogap state in underdoped samples. The pseudogap state between T_c and the temperature T^*, below which the gap in the low-energy excitation spectrum occurs, has been the subject of a wide range of theoretical proposals—from those focused on superconducting pairing correlations without phase coherence [1, 2] to those based on some form of competing electronic order or proximity to the Mott state [3–6]. Some experiments have shown evidence of pairing correlations above bulk T_c [7–10], while other experiments have associated the pseudogap with phenomena other than pairing, such as real space electronic organization, which is prominent at low doping [4, 11, 12].

One particular challenge in addressing these fundamental questions is the fact that, unlike conventional superconductors, cuprates are randomly doped systems with inherent atomic scale variations in their electronic and chemical structure. These variations complicate the interpretation of experiments that are averaged macroscopically and require the development of new techniques that enable precise measurements to determine when pairs are formed on the nanometer scale and whether there are specific aspects of the material's

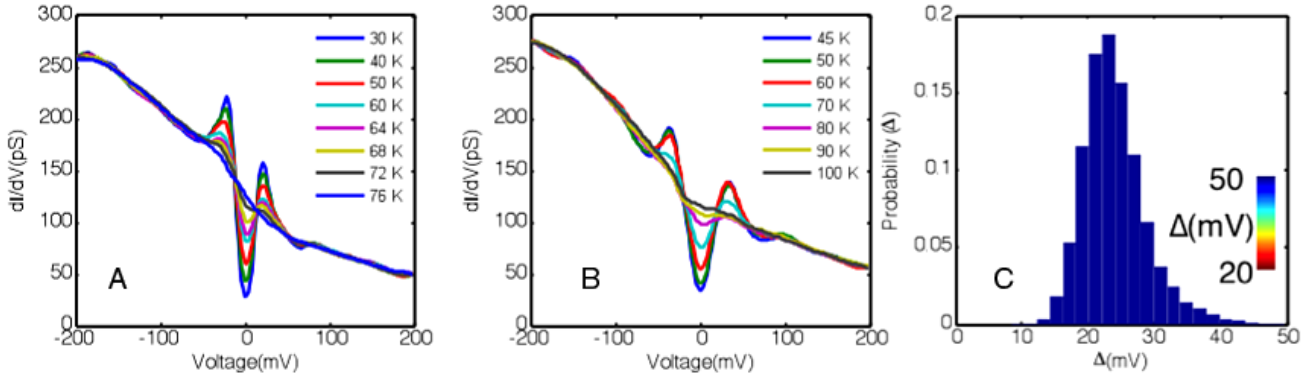

Figure 1. (A), (B) Temperature evolution of spectra at two atomic locations on an overdoped sample. (C) Distribution of gaps on the same sample at low temperatures.

properties (such as bosonic excitations) that control the strength of pairing. Here, I review the application of a newly developed lattice tracking spectroscopy technique with the scanning tunneling microscope (STM) to show that pairing gaps in $Bi_2Sr_2CaCu_2O_{8+\delta}$, in optimal and overdoped samples, nucleate in nanoscale regions at a temperature T_p above T_c [13]. These experiments provide a natural explanation of the signatures of fluctuating superconductivity above T_c, which have been reported in various experiments involving, for example, the Nernst effect and magnetization [8, 9]. They also provide an unprecedented view of the pairing process showing that, on average, the local pairing gaps and the temperature at which they first occur are related by the simple local relation: $2\Delta/k_BT_p \sim 8$. Finally, precision measurements of local electronic spectra can be used to show that the strength of pairing is independent of the coupling of electrons to bosonic excitations that leave prominent signatures on electron tunneling spectra [14]. Instead, we find that the strength of pairing is directly related to hole-like excitation that can be detected even in the correlated normal state of these compounds, well above when the pairs first form.

2. Lattice tracking spectroscopy: extracting the pairing gap

Electron tunneling spectroscopy of superconductors is a powerful method for quantitative measurement of the onset of electron pairing and the boson exchange mechanism in superconductors. The pioneering measurements of McMillan and Rowell [15] and the analysis [16] of the results (based on the extension of the BCS theory) by Eliashberg [17] provided unequivocal evidence for a phonon-mediated mechanism of superconductivity in metals and alloys. However, the success of tunneling as a quantitative spectroscopic probe in conventional superconductors relied on performing measurements in both the superconducting and normal state [18], which provides a method to exclude the complication due to tunneling matrix elements as well as inelastic tunneling processes. For an inhomogeneous superconductor, such as $Bi_2Sr_2CaCu_2O_{8+\delta}$, in which electronic states and the superconducting energy gap vary on the nanometer scale [19, 20], similar experiments pose a great technical challenge. To enable such measurements, it is necessary to track specific atomic locations on the lattice of the sample from low temperatures to temperatures above T_c using a scanning tunneling microscope (STM) [13]. Using a specially designed thermally compensated ultra-high vacuum STM system that can maintain thermal stability to better than ± 10 mK during experiments at high temperatures, we have developed these lattice tracking techniques up to temperatures of 110 K.

Figure 1 shows the use of the lattice tracking spectroscopy technique to measure the evolution of tunneling conductance $dI/dV(r, V, T)$ with temperature in overdoped samples of $Bi_2Sr_2CaCu_2O_{8+\delta}$ ($T_c = 68$ K, figures 1(A) and (B)) at two specific atomic sites. Spectra at different atomic sites show different energy gaps at low temperatures and evolve differently with increasing temperature. Figure 1(C) shows the distribution of the gap values in this overdoped sample. We find that all low temperature spectra in overdoped samples (figures 1(A) and (B)) evolve into spectra at high temperatures that are relatively featureless at low energies (<100 meV) and are independent of temperature. Following previous work on conventional superconductors [18], we probe the effects of superconductivity by examining the ratio $R(r, V, T) = [dI/dV]_N/[dI/dV]_S = N_S(r, V, T)/N_N(r, V, T)$ between the tunneling conductance in the superconducting and normal states measured under the same STM setup conditions. Here $N_S(r, V, T)$ and $N_N(r, V, T)$ are the respective normal and superconducting density of electronic states at atomic site r as a function of energy (eV). This ratio, which is independent of the tunneling matrix element, is used to extract the temperature dependence of the energy gap and features associated with strong coupling of electrons to bosonic modes.

The temperature evolution of the conductance ratio, $R(r, V, T)$, in overdoped $Bi_2Sr_2CaCu_2O_{8+\delta}$ samples at two representative locations of the sample with different low temperature energy gaps are shown in figures 2(A) and (B). Motivated by the fact that the low temperature ratio resembles that expected from a single energy gap in the spectrum, we compare these ratios with that expected from the thermally

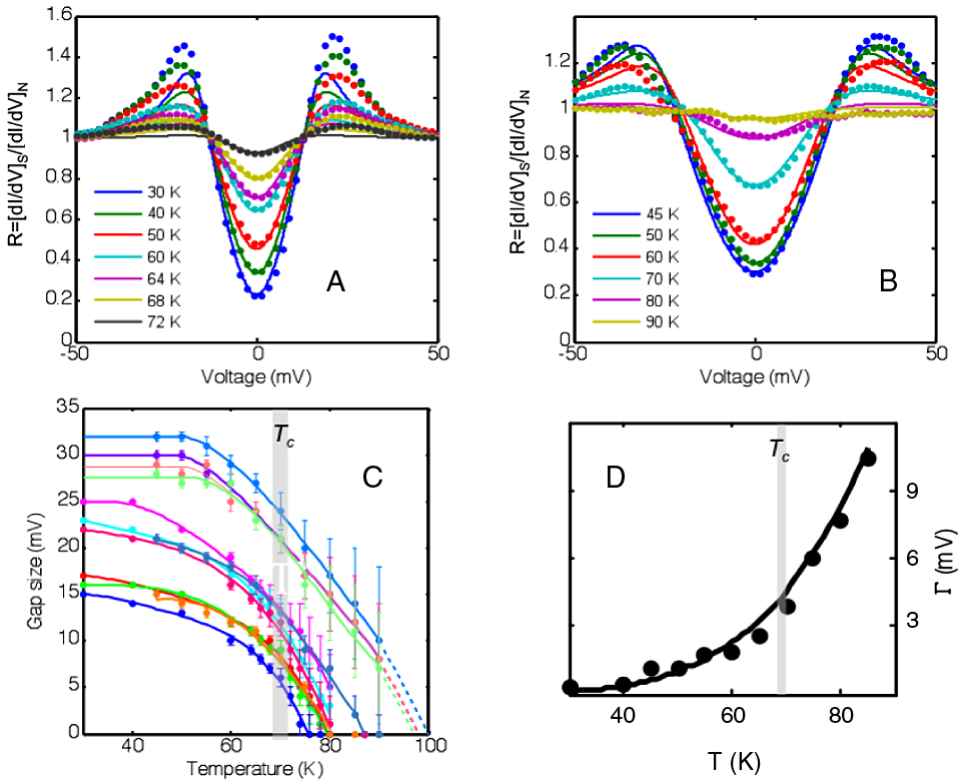

Figure 2. (A), (B) Temperature evolution of spectra at two points on an overdoped sample and fits to the model (1). (C) Temperature evolution of the pairing gap on an overdoped sample. (D) Temperature evolution of the inverse quasi-particle lifetime average over the overdoped sample.

broadened density of states of a d-wave superconductor:

$$\frac{N_S(r,V,T)}{N_N(r,V)} = \frac{1}{\pi}\int dE \frac{df(E+V,T)}{dE} \times \int_0^{\pi} d\theta \, \mathrm{Re}\frac{E - i\Gamma(r,T)}{\sqrt{(E - i\Gamma(r,T))^2 - \Delta(r,T)^2\cos^2 2\theta}}. \quad (1)$$

Here $\Delta(r,T)$ is the local gap (considered energy independent for low energies), $\Gamma(r,T)$ corresponds to the local inverse lifetime of the quasi-particle excitations [21] and $f(E,T)$ is the Fermi function. Such an analysis neglects the complication due to the k-dependence of the band structure as well as higher order angular terms in the superconducting gap. In general, we find that the model established by equation (1) provides an excellent fit to the experimental data at low energies (where the slope of R versus V is inversely proportional to the gap Δ) for all points on the overdoped samples (figures 2(A), (B)). Using this model, we can extract the local values of $\Delta(r,T)$ and $\Gamma(r,T)$ showing that at each point the gaps decrease monotonically with increasing temperature and close at a local temperature $T_p(r) > T_c$ (figure 2(C)). With increasing temperature, we find that the smaller gaps close first, with the largest gaps surviving to temperatures well above T_c. Clearly, $\Delta(r,T)$ is not affected by T_c. A signature of the loss of long range phase coherence can, however, be found in the average behavior of $\Gamma(r,T)$, which is much smaller than the gaps at all locations at low temperatures, but shows a dramatic rise at $T \sim T_c$ (figure 2(D)). This finding is consistent with the dramatic decrease of the quasi-particle lifetime at T_c as probed by many experiments on the cuprates over the years.

3. Visualizing gap formation: pairing gap and the phase diagram

The lattice tracking spectroscopy technique described above provides precise details of $\Delta(r,T)$ and evidence of the persistence of this gap above T_c. However, using the fact that we find $dI/dV(V=0) > dI/dV$ (for all $V > 0$) in the tunneling spectra when Δ is no longer measurable, we can develop a simple procedure that allows visualization of gap formation in our samples on the atomic scale. Spectra measured over large areas (~300 Å) of the samples as a function of temperature can be analyzed using the criterion above to create maps of gap values at different temperatures. While precise values of the gap are best measured from the lattice tracking spectroscopy technique, our focus here is to show that gaps survive in nanoscale regions at temperatures well above T_c, and their collapse in this temperature range is inhomogeneous. Examples of such measurements for an overdoped and optimally doped sample of $Bi_2Sr_2CaCu_2O_{8+\delta}$ are shown in figures 3(A) and (B), respectively. For the overdoped sample, the range of temperatures above T_c over which Δ is nonzero is relatively narrow; however, for an optimally doped sample, this range extends to about 50 K above T_c. It is also interesting to note that none of the gaps in the optimally doped sample disappear near T_c.

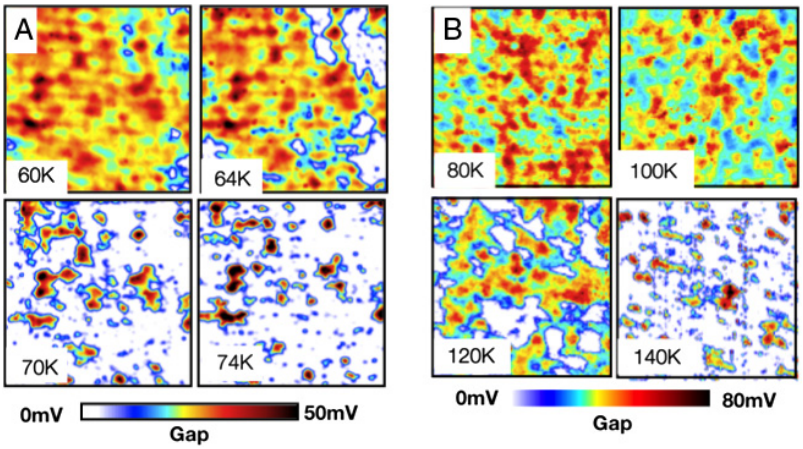

Figure 3. Inhomogeneous collapse of the gap in (A) an overdoped sample ($T_c = 65$ K) and (B) an optimally doped sample ($T_c = 93$ K).

As the lattice tracking spectroscopy measurements demonstrate, gaps measured to be larger at low temperature ($T \ll T_c$) persist to higher temperatures as compared to smaller gaps measured at the same temperature. Hence the distribution of the gapless regions at high temperature is related to the histogram of Δ at the lowest temperatures (see figure 1(C) for an example). Motivated by this observation, we have analyzed the data such as those in figures 3(A) and (B) to extract the relation between a given local Δ measured at $T \ll T_c$ and the temperature T_p at which it collapses. From the maps such as those shown in figure 3, we can extract the percentage of the sample that is gapped at a given temperature for samples with different doping levels (points in figure 4). To compare, we use the histogram of Δ values measured at the lowest temperature for each sample to compute the probability $P(<\Delta)$ that the gaps are less than a given Δ (solid line). A linear relationship between local Δ and T_p would require that the x axis of these two measurements be related by a simple ratio. We find that a relation $2\Delta/k_B T_p = 8.0 \pm 0.5$ can be used to collapse the data measured on all optimal and overdoped samples. This relation shows that despite the strong variation of the superconducting gaps on the nanoscale, as well as the difference between the average gap values between samples at different dopings, they all collapse following the same local criterion.

The fact that overdoped and optimally doped samples have identical gap–temperature scaling ratios, together with the excellent fits of the lattice tracking spectra with a single d-wave superconducting gap, implies that the collapsing gaps are indeed due to pairing. These results also show that, on average, pairing gaps and the temperature at which they close (which can be equal to or larger than T_c) follow a local criterion over a wide range of doping. The extracted ratio also shows that the local pairing gap is far more fragile to increases in temperature than are the conventional BCS superconductors, for which the ratio is in the range of 3.5–5. Surprisingly, the ratio is insensitive to the size of the gap, for gaps ranging from ~15 to 50 mV, indicating that even the smallest gaps are very far from the BCS limit.

Our ability to visualize the development of gaps together with the local pairing hypothesis which we have established

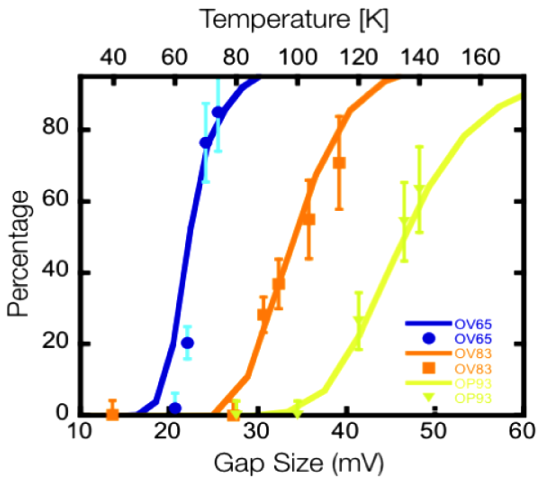

Figure 4. Finding scaling of T_p and Δ from a comparison of the percentage of ungapped regions for different samples (overdoped 63 K, 85 K and optimally doped 93 K) with the integral of gap distribution for each sample.

quantitatively on optimal and overdoped samples, provides a microscopic picture with which to understand several key aspects of the copper oxide phase diagram. In figure 5, we summarize our observations of the spatially inhomogeneous development of the gaps with a plot showing the percentage of areas that are gapped as a function of temperature and doping. In the various samples that we probed on the nanoscale, the rising percentage of gapped regions with lowering temperature correlates remarkably well with the onset of the suppression of low-energy excitations probed by other techniques [5]. As we discussed above, for the optimal and overdoped samples a single energy gap can describe all of our findings, strongly suggesting that the onset of the gap is indeed due to pairing, which occurs locally at T_p. The apparent T^* line on the overdoped side is controlled by the largest pairing gaps ($T_{p,max}$) for these samples. In addition, our data seem to suggest that when the percentage of gapped regions reaches roughly 50%, the Nernst and magnetization experiments register signatures of vortices and diamagnetism at T_o [8, 9].

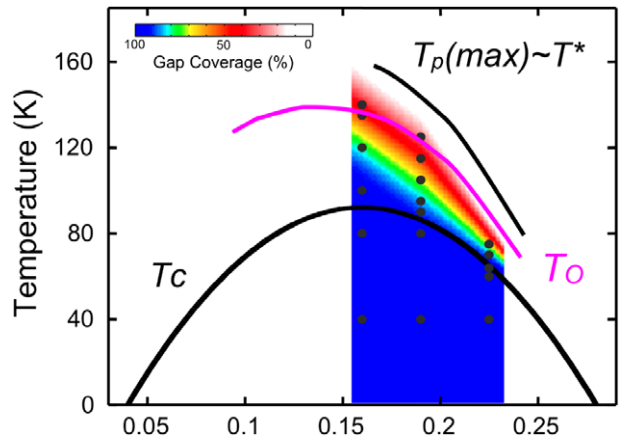

Figure 5. Phase diagram and percentage of gaps on various samples on the overdoped side. T_o presents the onset of Nernst and magnetization while T^* is the onset of pseudogap behavior.

For underdoped samples, it has been known for some time that the shape of the spectra does not follow a simple d-wave density of states, which makes it difficult to interpret the STM tunneling spectra based on the analysis described above [13]. This observation, together with the appearance of real space organization in electronic states, makes it difficult to separate the effects due to pairing and other potential ordering in underdoped samples [11, 12]. Currently, we are investigating this regime with temperature-dependent measurements of similar precision to determine the onset of pairing in underdoped samples.

4. Extracting coupling to bosonic mode from lattice tracking spectroscopy

Having established that the pairs in optimal and overdoped $Bi_2Sr_2CaCu_2O_{8+\delta}$ samples nucleate in small nanoscale regions above T_c, we can turn our attention to the question of what controls the strength of the pairing gap locally. It is unlikely that the pairing mechanism in the overdoped samples is different from that in the underdoped samples; hence, precise measurements on overdoped samples can be used to draw conclusions about the mechanism of pairing. In section 2, we have already demonstrated that our lattice tracking spectroscopic measurements on overdoped samples can be examined within the context of a local d-wave gap model in equation (1), so now we analyze the deviation of the conductance ratio from this model for $E > \Delta$. Although other effects such as inelastic tunneling [18, 22] can cause such deviations, only strong coupling of electrons to bosonic modes is known to cause the superconducting state tunneling conductance to dip strongly below the normal state [16, 18]. As illustrated in figure 6(A), all points on the samples show a voltage range (around 50–80 meV) in which the conductance ratio $R(r, V, T)$ is reduced below 1 and show systematic deviations from the local d-wave model. Analogous to previous work on conventional superconductors [23], these deviations provide a quantitative method to determine the strength of electron–boson coupling. The analysis of the spectra based on the features of $R(r, V, T)$ instead of the bare $dI/dV(r, V, T)$ or $dI^2/dV^2(r, V, T)$ avoids complications due to the spatial variation of normal state features and variations in the tunneling matrix element [24]. Although many previous studies, including those using an STM [25], have examined electron–boson features in the 20–120 meV range, a quantitative comparison of the electron–boson coupling at different locations of the sample with different pairing gaps has not been accomplished. The comparison of $R(r, V, T)$ at different locations allows us to quantitatively evaluate the role of bosonic features in the development of the pairing gaps and their inhomogeneity.

To study the relative strength of electron–boson coupling at different locations on the sample, we consider that the strong

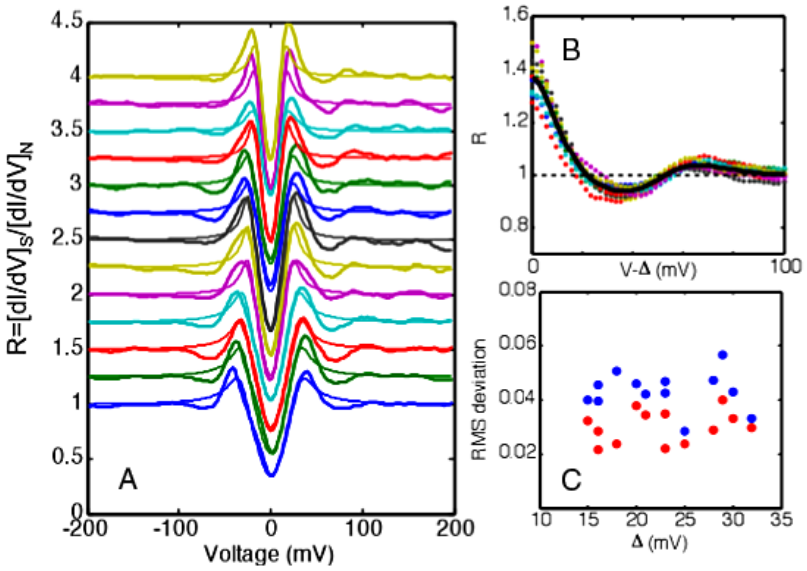

Figure 6. (A) Conductance ratio and d-wave fits for different locations on the overdoped sample. (B) Collapse of the positive bias part of the curves in (A) when plotted with respect to the local gap. (C) RMS deviation between the fit and the data as a function of local gap size.

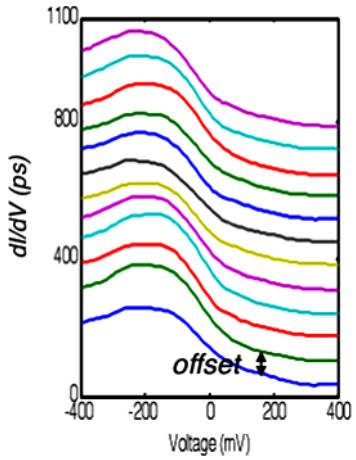

Figure 7. Normal state tunneling spectra for an overdoped sample at $T > 90$ K. Different spots show varying spectra but similar electron–hole asymmetry.

coupling to a bosonic mode at energy Ω in a superconductor results in features in the conductance ratio at $eV = \Delta + \Omega$ [18, 26, 27]. Since the pairing gap is locally varying, we plot $R(r, V, T)$ as a function of $eV - \Delta(r)$ for different atomic sites on the sample with low temperature $\Delta(r)$ ranging between 15 and 32 meV, as shown in figure 6(B). This figure demonstrates that different locations on the sample show remarkably similar $R(r, V, T)$ curves in magnitude and shape, once we take into account their varying pairing gaps. A quantitative measurement of the strength of the local coupling constant is the RMS deviation of $R(r, V, T)$ from the weak-coupling d-wave model (equation (1)) in the energy range 20–120 meV beyond the gap. These deviations show no correlation (for both positive and negative biases, figure 6(C)) with the size of the local gap within our experimental error.

For boson-mediated pairing, variation of the pairing gap can be caused by changes in either the local boson energy or the local coupling between the boson and electrons [23]. Such changes are reflected directly in the size and energy range of the strong-coupling features in the conductance ratio. Since both the energy scale of the boson modes and the local electron–boson coupling do not correlate strongly with the magnitude of the local pairing gap in our samples, we are forced to conclude that the coupling to bosons in the range of 20–120 meV cannot be responsible for these inhomogeneous pairing gaps.

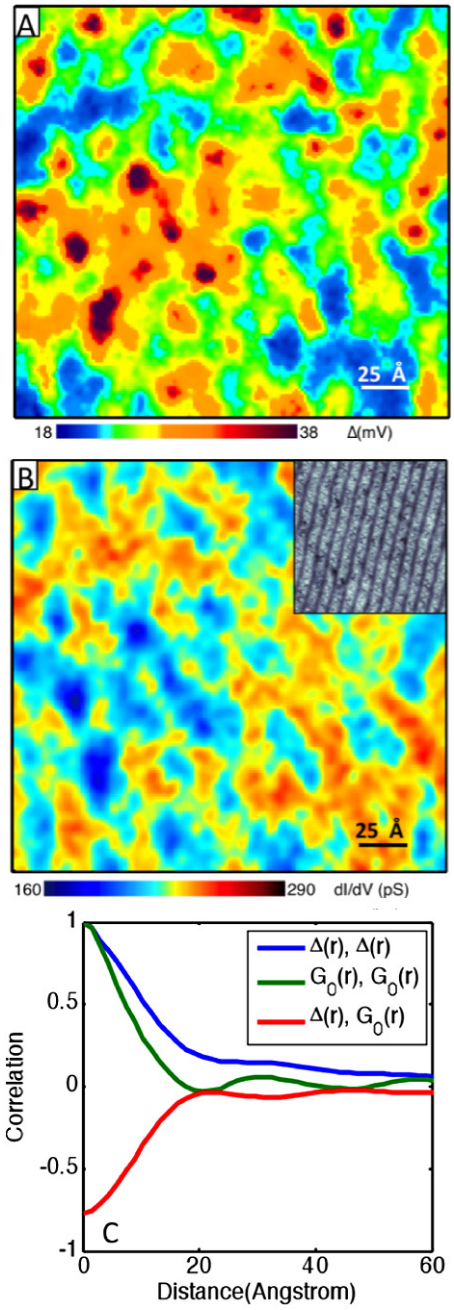

Figure 8. (A) Gap map measured over a region of an overdoped sample ($T_c = 68$ K). (B) Conductance map at the Fermi energy over the exact same region as in (A). The inset to this figure also shows a topograph of the same area. (C) Auto-correlation of the maps in (A) and (B) as well as their cross-correlation.

5. Normal state clues on the pairing mechanism

In search of the origin of the pairing interaction in the cuprates, we focus on spectroscopic measurements of the electronic excitations in the normal state and their correlation with the spatially inhomogeneous pairing strength in the superconducting state. To reach the normal state, the temperature has to be high enough such that all the local pairing gaps have collapsed. For overdoped $Bi_2Sr_2CaCu_2O_{8+\delta}$ samples (hole doping $x = 0.24$, $T_c = 62$ K), less than 1% of the sample shows a gap at 90 K. In the intermediate temperature between T_c and 90 K, these samples show a mixture of ungapped and partially gapped spectra, as previously reported [13]. Above 90 K, the tunneling spectra are gapless at all locations on the sample but show asymmetric behavior for electron and hole tunneling. Careful examination of these spectra, over a wide range of energies, shows that electronic excitations in the sample are still spatially inhomogeneous at temperatures well above the temperature at which pairs first form in the sample (see figure 7, for example).

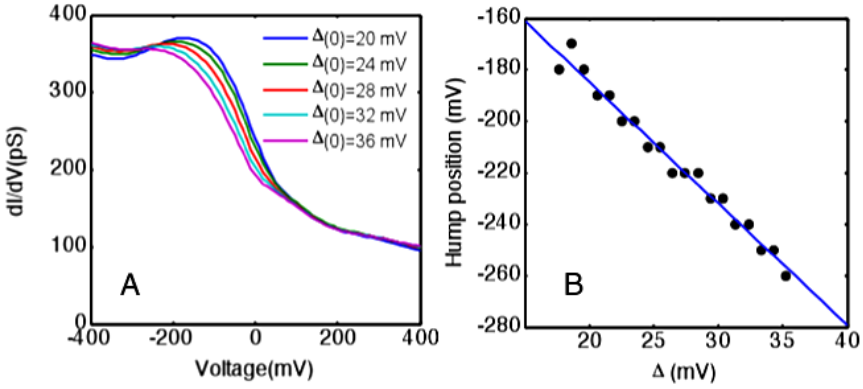

Figure 9. (A) Measured normal state conductance map averaged for regions that develop the same pairing gap at low temperatures. (B) Location of the hump in energy in spectra in (A) plotted versus gap size.

A comparison of the gap map in the superconducting state measured at 30 K with the normal state conductance map measured at the Fermi energy on the exact same area of the sample reveals a remarkable correlation. As illustrated by the data in figures 8(A) and (B), regions of the sample with a lower normal state conductance at the Fermi level nucleate superconducting gaps at higher temperatures, resulting in larger low temperature gaps. Quantifying these correlations in figure 8(C), we show that the normal state conductance map and the low temperature gap map are strongly anti-correlated (-0.75). Further, both of these maps have very similar auto-correlation lengths, indicating that the spatial variation of the normal state is intimately linked to that of the low temperature gap. These measurements show that the variation of the superconducting state in $Bi_2Sr_2CaCu_2O_{8+\delta}$ samples, which for typical superconductors is characterized by a temperature-dependent superconducting coherence length, appears to be for the most part determined by the spatial variation of the normal state at high temperatures.

Since our measurements show that the spatial variation of the normal state conductance and the low temperature pairing gap maps are intimately connected, we can associate an average normal state spectrum with a low temperature gap value. We thus average together normal state spectra of regions of the sample that show identical low temperature gaps and plot these average spectra in figure 9(A). As this figure shows, systematic differences in the normal state spectra foreshadow the eventual variation of the gap in the superconducting state. In particular, the systematic shift of a hump in the normal state tunneling spectra at negative bias, in the range of -150 to -300 meV (figure 9(B)), as well as the value of tunneling conductance at the Fermi energy, track the size of the superconducting gap observed at low temperatures. An important point illustrated by the data in figure 9 is that the hole-like excitations in the normal state are somehow critical to determining the size of the pairing gap.

It is important to compare our measurements of the normal state with those obtained from other spectroscopic techniques. In both angle-resolved photoemission (ARPES) and optical spectroscopy, strong renormalization of the single-particle excitations has been observed over an energy range of $\sim$200–400 meV below the Fermi energy in $Bi_2Sr_2CaCu_2O_{8+\delta}$ samples [27–34]. Such effects have been previously interpreted as either due to the coupling of electrons with a spectrum of bosonic excitations (such as spin fluctuations) or as a consequence of the energy band structure (such as the bilayer splitting) of this compound [30, 35]. It is difficult to associate the normal state features that we measure with coupling to bosonic excitations due to their strong electron–hole asymmetry. Although we strictly cannot rule out bosonic excitations as the origin of these features, candidate bosons would have to couple very asymmetrically to the tunneling of electrons and holes. Assigning these features to effects calculated from a simple non-interacting bandstructure can also be questioned given both the strong spatial variation at the atomic scale of the normal state spectra reported here and the strong renormalization of single-particle states at similar energies in other spectroscopic studies of the normal state. Instead, these features might be the excitations of a doped Mott insulator where the electron and hole excitations are naturally asymmetric as a consequence of the strong Coulomb interaction [36–38]. Although there is no clear consensus on a model for these excitations, our experiments show that the spectroscopic features of this state are indeed the origin of the nanoscale variation of the pairing strength in the superconducting state.

Finally, we address the question of the underlying cause of variations of the normal state excitations in $Bi_2Sr_2CaCu_2O_{8+\delta}$ samples. Our analysis finds that both structural and electronic features of the samples contribute to such variations. We find that there are small correlations (about 10%) of the normal state conductance maps with the structural supermodulation along the *b*-axis in these samples. Similarly, we find that maps of electronic resonances around -900 meV previously probed in similar samples with STM [39] are correlated with the normal state conductance maps (about 30%) [14]. Our measurements show that structural and chemical inhomogeneity affects both the excitations of the normal state and the superconducting gap.

6. Conclusion

The overall picture emerging from the results described here is that pairing in the $Bi_2Sr_2CaCu_2O_{8+\delta}$ samples nucleates over a broad range of temperatures above T_c. The growth and proliferation of these nanoscale regions is directly connected with the phase diagram and the Nernst and magnetization signal measured on the same material systems. The consistency between these findings strongly suggests that the onset of the resistive transition is controlled by phase coherence and not the formation of pairs. Although a complete understanding of the phase coherence onset and a detailed model of such a phenomena in cuprates is still lacking, the quasi-particle lifetime probed in our spectroscopic measurements in the cuprates here and in other measurements over the years is consistent with sudden onset of the fluctuations of the phase of the order parameter at T_c.

From another perspective, we have used the spatial variation of the pairing gaps, which gives rise to a range of pairing temperatures in nanoscale regions of our samples above T_c, as a diagnostic tool to find clues to the underlying mechanism of superconductivity. Temperature-dependent lattice tracking spectroscopy has allowed us to demonstrate that electron–boson coupling in the 20–120 meV range does not cause the variation of pairing gaps and onset temperatures in our samples. In contrast, we find that the high-energy (up to ∼400 mV) hole-like excitations of the normal state are a direct predictor of the strength of pairing and its spatial variation. The anti-correlation between the normal state conductance at the Fermi level and local strength of pairing also runs contrary to a BCS-like pairing mechanism where the coupling to bosons is proportional to the density of states at the Fermi energy [23]. Overall, the conclusion of these experiments points to the importance of electronic correlation responsible for the asymmetric hump in the normal state conductance, as opposed to low-energy bosonic excitations.

Acknowledgments

I thank my collaborators A Pasupathy, A Pushp, K Gomes, C Parker, G Gu, S Ono and Y Ando. This work has been supported by DOE and NSF through the Princeton Center for Complex Materials.

References

[1] Emery V J and Kivelson S A 1995 Importance of phase fluctuations in superconductors with small superfluid density *Nature* **374** 434–7

[2] Randeria M 1998 *Int. School of Physics 'Enrico Fermi' on Conventional and High Temperature Superconductors: Proc. Int. School of Physics 'Enrico Fermi' on Conventional and High Temperature Superconductors* (Amsterdam: IOS Press)

[3] Tallon J L and Loram J W 2001 The doping dependence of T^*—what is the real high-t-c phase diagram? *Physica* C **349** 53–68

[4] Kivelson S A, Bindloss I P, Fradkin E, Oganesyan V, Tranquada J M, Kapitulnik A and Howald C 2003 How to detect fluctuating stripes in the high-temperature superconductors *Rev. Mod. Phys.* **75** 1201–41

[5] Norman M R, Pines D and Kallin C 2005 The pseudogap: friend or foe of high t_c? *Adv. Phys.* **54** 715–33

[6] Lee P A, Nagosa N and Wen X-G 2006 Doping a Mott insulator: physics of high-temperature superconductivity *Rev. Mod. Phys.* **78** 17–86

[7] Xu Z A, Ong N P, Wang Y, Kakeshita T and Uchida S 2000 Vortex-like excitations and the onset of superconducting phase fluctuation in underdoped $La_{2-x}Sr_xCuO_4$ *Nature* **406** 486–8

[8] Wang Y Y, Li L, Naughton M J, Gu G D, Uchida S and Ong N P 2005 Field-enhanced diamagnetism in the pseudogap state of the cuprate $Bi_2Sr_2CaCu_2O_{8+\delta}$ superconductor in an intense magnetic field *Phys. Rev. Lett.* **95** 247002

[9] Wang Y, Lu L and Ong N P 2006 Nernst effect in high-t_c superconductors *Phys. Rev.* B **73** 024510

[10] Corson J, Mallozzi R, Orenstein J, Eckstein J N and Bozovic I 1999 Vanishing of phase coherence in underdoped $Bi_2Sr_2CaCu_2O_{8+\delta}$ *Nature* **398** 221–3

[11] Vershinin M, Misra S, Ono S, Abe Y, Ando Y and Yazdani A 2004 Local ordering in the pseudogap state of the high-t_c superconductor $Bi_2Sr_2CaCu_2O_{8+\delta}$ *Science* **303** 1995–8

[12] Hanaguri T, Lupien C, Kohsaka Y, Lee D H, Azuma M, Takano M, Takagi H and Davis J C 2004 A 'checkerboard' electronic crystal state in lightly hole-doped $Ca_{2-x}Na_xCuO_2Cl_2$ *Nature* **430** 1001–5

[13] Gomes K K, Pasupathy A N, Pushp A, Ono S, Ando Y and Yazdani A 2007 Visualizing pair formation on the atomic scale in the high-t_c superconductor $Bi_2Sr_2CaCu_2O_{8+\delta}$ *Nature* **447** 569–72

[14] Pasupathy A N, Pushp A, Gomes K K, Parker C V, Wen J S, Xu Z J, Gu G D, Ono S, Ando Y and Yazdani A 2008 Electronic origin of the inhomogeneous pairing interaction in the high-t-c superconductor $Bi_2Sr_2CaCu_2O_{8+\delta}$ *Science* **320** 196–201

[15] McMillan W L and Rowell J M 1965 Lead phonon spectrum calculated from superconducting density of states *Phys. Rev. Lett.* **14** 108

[16] Scalapino D J, Schrieffer J R and Wilkins J W 1966 Strong-coupling superconductivity. I *Phys. Rev.* **148** 263–79

[17] Eliashberg G M 1960 Interactions between electrons and lattice vibrations in a superconductor *Sov. Phys.—JETP-USSR* **11** 696–702

[18] McMillan W L and Rowell J M 1969 *Superconductivity* ed R D Parks (New York: Dekker) pp 561–613

[19] Howald C, Fournier R and Kapitulnik A 2001 Inherent inhomogeneities in tunneling spectra of $Bi_2Sr_2CaCu_2O_{8-x}$ crystals in the superconducting state *Phys. Rev.* B **64** 100504(R)

[20] Pan S H *et al* 2001 Microscopic electronic inhomogeneity in the high-t_c superconductor $Bi_2Sr_2CaCu_2O_{8+x}$ *Nature* **413** 282–5

[21] Dynes R C, Narayanamurti V and Garno J P 1978 Direct measurement of quasiparticle-lifetime broadening in a strong-coupled superconductor *Phys. Rev. Lett.* **41** 1509–12

[22] Pilgram S, Rice T M and Sigrist M 2006 Role of inelastic tunneling through the insulating barrier in scanning-tunneling-microscope experiments on cuprate superconductors *Phys. Rev. Lett.* **97** 117003

[23] Carbotte J P 1990 Properties of boson-exchange superconductors *Rev. Mod. Phys.* **62** 1027–157

[24] Scalapino D J 2006 Superconductivity—pairing glue or inelastic tunnelling? *Nat. Phys.* **2** 593–4

[25] Lee J *et al* 2006 Interplay of electron-lattice interactions and superconductivity in $Bi_2Sr_2CaCu_2O_{8+\delta}$ *Nature* **442** 546–50

[26] Zhu J X, Balatsky A V, Devereaux T P, Si Q M, Lee J, McElroy K and Davis J C 2006 Fourier-transformed local density of states and tunneling into a d-wave superconductor with bosonic modes *Phys. Rev.* B **73** 014511

[27] Eschrig M and Norman M R 2003 Effect of the magnetic resonance on the electronic spectra of high-t_c superconductors *Phys. Rev.* B **67** 144503

[28] Campuzano J C, Norman M R and Randeria M 2003 *The Physics of Superconductors* ed K H Bennemann and J B Ketterson (Berlin: Springer) pp 167–265
[29] Cuk T, Lu D H, Zhou X J, Shen Z X, Devereaux T P and Nagaosa N 2005 A review of electron–phonon coupling seen in the high-t_c superconductors by angle-resolved photoemission studies (arpes) *Phys. Status Solidi* b **242** 11–29
[30] Fink J 2007 *Very High Resolution Photoelectron Spectroscopy* ed S Hüfner (New York: Springer) pp 295–325
[31] Hwang J, Nicol E J, Timusk T, Knigavko A and Carbotte J P 2007 High energy scales in the optical self-energy of the cuprate superconductors *Phys. Rev. Lett.* **98** 207002
[32] van der Marel D, Molegraaf H J A, Zaanen J, Nussinov Z, Carbone F, Damascelli A, Eisaki H, Greven M, Kes P H and Li M 2003 Quantum critical behaviour in a high-t_c superconductor *Nature* **425** 271
[33] Meevasana W *et al* 2007 Hierarchy of multiple many-body interaction scales in high-temperature superconductors *Phys. Rev.* B **75** 174506
[34] Graf J *et al* 2007 Universal high energy anomaly in the angle-resolved photoemission spectra of high temperature superconductors: possible evidence of spinon and holon branches *Phys. Rev. Lett.* **98** 067004
[35] Damascelli A, Hussain Z and Shen Z X 2003 Angle-resolved photoemission studies of the cuprate superconductors *Rev. Mod. Phys.* **75** 473–541
[36] Meinders M B J, Eskes H and Sawatzky G A 1993 Spectral-weight transfer—breakdown of low-energy-scale sum-rules in correlated systems *Phys. Rev.* B **48** 3916–26
[37] Randeria M, Sensarma R, Trivedi N and Zhang F C 2005 Particle–hole asymmetry in doped Mott insulators: implications for tunneling and photoemission spectroscopies *Phys. Rev. Lett.* **95** 137001
[38] Anderson P W 2006 The 'strange metal' is a projected Fermi liquid with edge singularities *Nat. Phys.* **2** 626
[39] Mcelroy K, Lee J, Slezak J A, Lee D H, Eisaki H, Uchida S and Davis J C 2005 Atomic-scale sources and mechanism of nanoscale electronic disorder in $Bi_2Sr_2CaCu_2O_{8+\delta}$ *Science* **309** 1048–52